

# Thermal trimming and tuning of hydrogenated amorphous silicon nanophotonic devices

Shankar Kumar Selvaraja,<sup>1,a)</sup> Wim Bogaerts,<sup>1</sup> Dries VanThourhout,<sup>1</sup> and Marc Schaekers<sup>2</sup>

<sup>1</sup>Department of Information Technology, Photonic research group, Ghent University-IMEC, Ghent 9000, Belgium

<sup>2</sup>IMEC, Leuven 3001, Belgium

(Received 7 May 2010; accepted 16 July 2010; published online 20 August 2010)

Deposited silicon and, in particular, hydrogenated amorphous silicon forms an attractive alternative platform for realizing compact photonic integrated circuits. In this paper we report on trimming (toward lower wavelengths) and tuning (toward higher wavelengths) of photonic devices through a suitable thermal treatment. The former is achieved by a material density change, the latter through the thermo-optic effect. By using Fourier transform infrared spectroscopy, a change in the hydrogen content is identified as the source of the density change. A total wavelength tuning range of 24.6 nm is achievable, which can be used for compensating fabrication imperfections. © 2010 American Institute of Physics. [doi:10.1063/1.3479918]

The use of deposited silicon layers instead of crystalline silicon-on-insulator wafers forms an attractive alternative for realizing compact integrated photonic devices.<sup>1,2</sup> Recently, we have demonstrated low-loss photonics wires and wavelength selective devices fabricated in hydrogenated amorphous silicon (a-Si:H).<sup>1</sup> Plasma enhanced chemical vapor deposition (PECVD) with SiH<sub>4</sub> as the precursor is widely used for achieving a low-loss guiding layer for photonic applications. Because of the reduced process temperature, PECVD deposition is a promising process for integrating photonics circuits on top of prefabricated electronic circuits, since this imposes strong constraints on the processing and operating temperature (<400 °C). In addition, the PECVD process allows for dangling bond reduction during the deposition process through hydrogen passivation of the film. The properties of a-Si:H, such as the refractive index and crystallinity are strongly influenced by the amount of hydrogen (H) incorporated in the film, and can be controlled by process parameters, such as the substrate temperature, the rf power and the gas flow rate. When the film is in thermodynamic equilibrium, the H in an a-Si:H network manifests itself in different configurations (SiH<sub>x=1-3</sub>) and bond energies. If the equilibrium in the film is disturbed optically<sup>3,4</sup> or thermally,<sup>5-7</sup> bond breaking and reorganization of the network occurs.<sup>8</sup> This results in hydrogen desorption and crystallization. Despite considerable material development, there are no reports on the thermal properties of a-Si:H used for photonic integrated circuits.

In this paper, we present the effects of a thermal treatment on propagation loss and refractive index change of photonic devices fabricated in a-Si:H. The devices were annealed at high temperatures (150–600 °C) followed by optical characterization at room temperature. The material compositional changes were studied using Fourier transform infrared spectroscopy (FTIR) and compared with the device characteristics. In addition, the devices were characterized at elevated temperatures to measure the thermo-optic (TO) effect of a-Si:H. Finally, we present an approach to use the

thermal properties of a-Si:H for compensating fabrications imperfection of the devices.<sup>9</sup>

The thermal effect of a-Si:H was studied by using two types of photonic devices: Mach-Zehnder interferometers (MZIs) and long spiral waveguides (Fig. 1). The MZI is used to determine refractive index changes by measuring the spectral response of the device. The spiral waveguides are used to characterize material absorption losses, which can be estimated from the waveguide propagation loss. The 1 × 1 MZI was composed of two connected Y-splitters with a delay length ( $\delta L$ ) of 50  $\mu\text{m}$  in one of the two arms [Fig. 1(a)]. The spiral photonic wires of varying length (0.5 to 40 cm) were realized using straight and bend waveguides. Large bending radii (20  $\mu\text{m}$ ) were used to avoid any bend loss. The cross section of the photonic wire was 450 × 220 nm<sup>2</sup>, resulting in single mode waveguides.

We fabricated the devices on a 200 mm wafer with 220 nm of low-loss a-Si:H (Ref. 1) as the waveguiding layer. The waveguide layer was deposited using a PECVD process on top of 2000 nm surface polished high-density plasma silicon dioxide. After layer deposition, the photonic devices were fabricated using 193 nm optical lithography and dry etching.<sup>10</sup> Next the wafer was diced into individual samples. Then the devices in the different samples were optically characterized to obtain the reference spectral response and propagation loss. The optical characterization was done by injecting TE polarized broadband (1500–1600 nm) light from a superluminescent light emitting diode and measuring the output through an optical spectrum analyzer. Identical grating fiber-chip couplers were used for in and out coupling

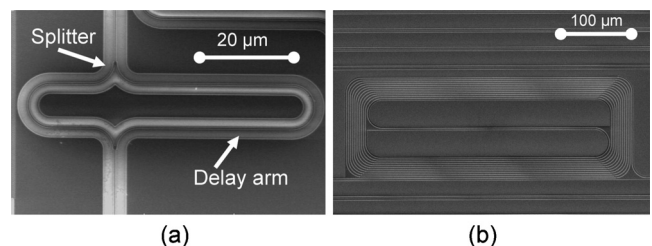


FIG. 1. One of the fabricated MZI and spiral photonic wire waveguide.

<sup>a)</sup>Electronic mail: shankar@intec.ugent.be.

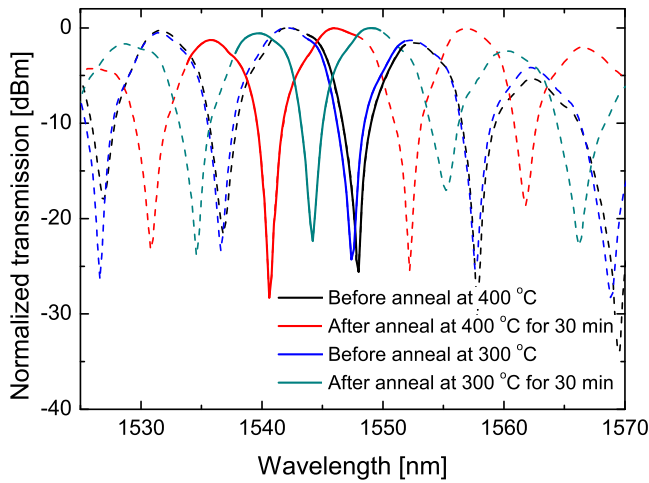


FIG. 2. (Color online) Transmission spectrum of MZI before and after annealing at 300 and 400 °C. The continuous lines show one free spectral range for clarity.

of light.<sup>11</sup> After reference measurements, each sample was annealed at different temperatures ranging from 100 to 600 °C for 30 min in a nitrogen ambiance. To avoid thermal shock, the samples were loaded and unloaded at clean room temperature, while the raise and fall temperature was set at 10 °C/min. Finally, the annealed samples were optically characterized again at room temperature. In addition, unannealed samples were characterized at elevated temperatures to measure the TO effect.

As shown in Fig. 2, we observe a blueshift in the spectral response of the MZI's after annealing. The observed spectral shift is a consequence of a reduction in the effective refractive index ( $N_{\text{eff}}$ ) of the photonic wire. Through numerical simulations using scattering matrix method, we have found that 1 nm wavelength shift corresponds to a change of  $2.9 \times 10^{-3}$  in the effective refractive index of the zeroth order guided mode (Fig. 3).

The measured wavelength shift follows a linear trend beyond a critical temperature ( $T_c$ ) of 200 °C (Fig. 4) reaching a maximum shift of  $-6.6$  nm at 400 °C. However, below the critical temperature  $T_c$  no wavelength response is observed. Due to the strongly increasing propagation loss, we

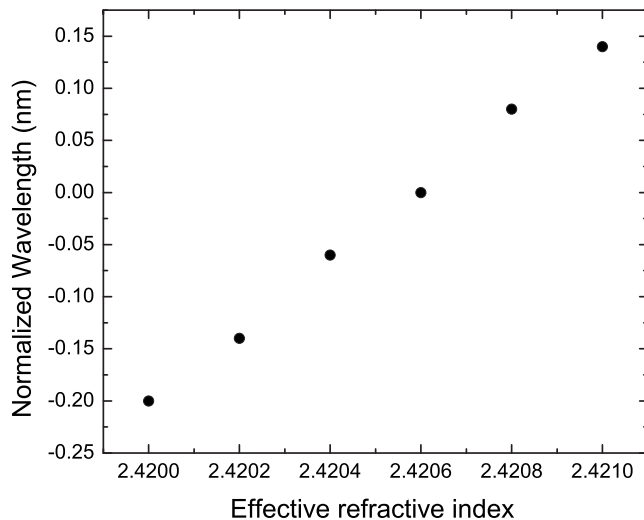


FIG. 3. Simulated spectral shift of a MZI as a function of effective refractive index of the photonic wire.

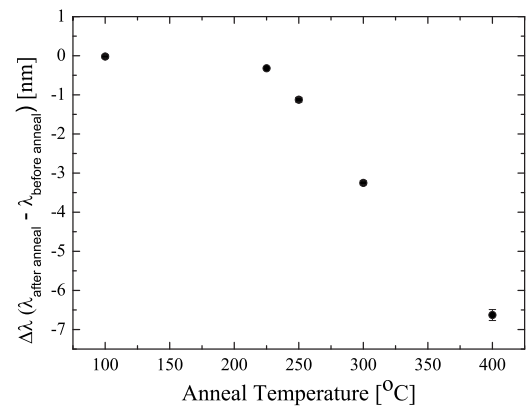


FIG. 4. Effect of anneal temperature on spectral shift of MZI.

were unable to measure samples annealed above 400 °C. However, for temperatures below 400 °C the loss did not vary beyond 0.2 dB/cm (Fig. 5).

The change in the spectral response and the propagation loss can be directly related to permanent change in the material property of a-Si:H after annealing. The amount of H in a silicon network affects the properties of the a-Si:H film, including the film density. It is well known that at an elevated temperature the mobility of H in the film increases, resulting in desorption of H from the Si network.<sup>5</sup> The two main consequences of H desorption are decrease in refractive index and creation of Si dangling bonds. The three important FTIR phonon mode bands related to the different Si-H bond configurations are located at 640, 2000, and 2100  $\text{cm}^{-1}$ . Figures 6 and 7 show the integrated intensity and the absorption spectra for Si-H monohydride at 2000 and 640  $\text{cm}^{-1}$ . It is obvious from these figures that the intensity of the 2000 and 640  $\text{cm}^{-1}$  peaks starts to decrease beyond the critical temperature  $T_c$ . This clearly indicates that the observed wavelength shift is a result of H desorption. As mentioned earlier, Si dangling bond are created due to the loss of H. As a consequence, the propagation loss is expected to increase due to absorption. Despite this, we did not observe a considerable change in the propagation loss up to 400 °C (Fig. 5). This suggests a reorganizing mechanism<sup>8</sup> in the network below 400 °C, which reduces the dangling bond density. Beyond 400 °C loss of most H atoms (Figs. 6 and 7) results in a high dangling bond density and a very high propagation loss.

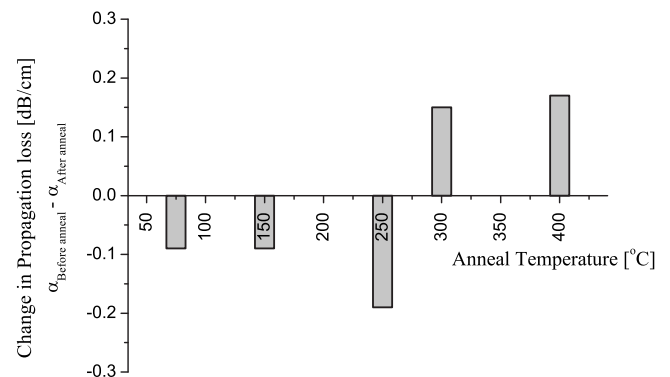
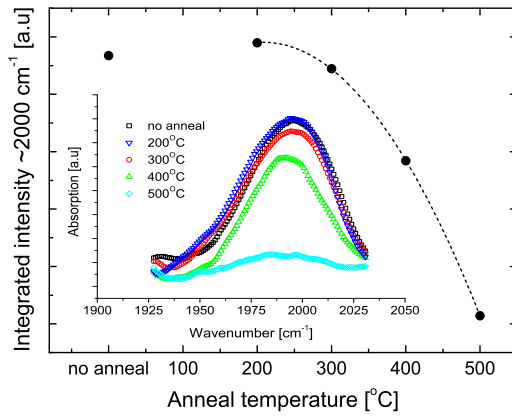


FIG. 5. Change in propagation loss of photonic wires as a function of anneal temperature.

FIG. 6. (Color online) (●) FTIR spectrum at 2000  $\text{cm}^{-1}$ .

The critical temperature ( $T_c$ ) clearly demarks two regions; a chemically stable ( $<T_c$ ) and an unstable ( $>T_c$ ) operating region. These two regions can be used to carry out a postfabrication compensation of fabrication inaccuracies. It is clear from our experiments that above  $T_c$  the devices can be trimmed toward lower wavelength. On the other hand, since the material is chemically stable below  $T_c$ , in this region the TO effect can be exploited to tune the device toward higher wavelengths. Due to the positive TO coefficient,<sup>12</sup> we observe a redshift of 90  $\text{pm}/^\circ\text{C}$  ( $d\lambda/dT$ ). This is illustrated in Fig. 8, which shows the wavelength shift of a MZI as function of the operating temperature. The total achievable tuning then ranges from  $-6.6$  to  $+18$  nm.

In conclusion, we have studied the effect of a thermal treatment on PECVD deposited a-Si:H films by characterizing photonic integrated devices. We have identified a critical temperature, which demarks two temperature ranges allowing for nonpermanent (tuning), respectively, permanent (trimming) changing of the material properties. By annealing

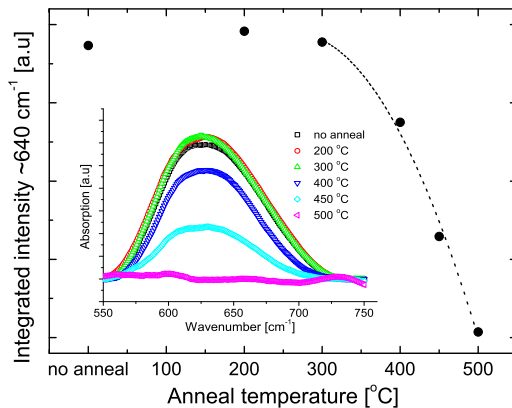
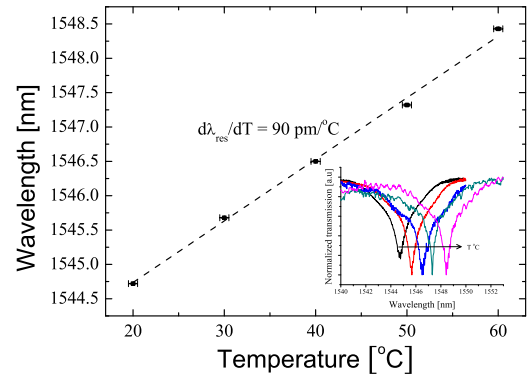
FIG. 7. (Color online) (●) FTIR spectrum at 640  $\text{cm}^{-1}$ .

FIG. 8. (Color online) TO effect of a-Si:H, inset shows the spectral shift of a MZI at different temperatures.

as-fabricated devices, we achieved trimming of wavelength selective photonic devices upto 6.6 nm. In this case, the wavelength response was blueshifted. Despite this change, the propagation loss of the photonic wire waveguides did not change more than 0.2 dB/cm. Through FTIR spectroscopy, we showed that this trimming effect is a consequence of hydrogen loss during annealing. In addition, by using the TO effect, we demonstrated thermal tuning of 90  $\text{pm}/^\circ\text{C}$ . We believe that in combination, trimming and tuning can be used to solve fabrication inaccuracies<sup>9</sup> in Si photonic devices fabricated in a-Si:H films.

This work was partly supported by the European Union through the ICT-WADIMOS project and through the Dutch Smartmix program Memphis.

- <sup>1</sup>S. K. Selvaraja, E. Slecckx, M. Schaekers, W. Bogaerts, D. Van Thourhout, P. Dumon, and R. Baets, *Opt. Commun.* **282**, 1767 (2009).
- <sup>2</sup>D. K. Sparacin, R. Sun, A. M. Agarwal, M. A. Beals, J. Michel, L. C. Kimmerling, T. J. Conway, A. T. Pomerene, D. N. Carothers, M. J. Grove, D. M. Gill, M. S. Rasras, S. S. Patel, and A. E. White, *Low loss amorphous silicon channel waveguides for integrated photonics*, *3rd IEEE International Conference on Group IV Photonics* (IEEE, Ottawa, Ontario, Canada, 2006), p. 255.
- <sup>3</sup>J. M. Pearce, J. Deng, R. W. Collins, and C. R. Wronski, *Appl. Phys. Lett.* **83**, 3725 (2003).
- <sup>4</sup>D. Han, J. Baugh, G. Yue, and Q. Wang, *Phys. Rev. B* **62**, 7169 (2000).
- <sup>5</sup>W. Beyer and H. Wagner, *J. Phys.* **42**, 783 (1981).
- <sup>6</sup>T. Sakka, K. Toyoda, and M. Iwasaki, *Appl. Phys. Lett.* **55**, 1068 (1989).
- <sup>7</sup>W. C. Hsiao, C. P. Liu, and Y. L. Wang, *J. Phys. Chem. Solids* **69**, 648 (2008).
- <sup>8</sup>H. M. Branz and E. Iwaniczko, *Phys. Rev. B* **48**, 17114 (1993).
- <sup>9</sup>S. K. Selvaraja, W. Bogaerts, P. Dumon, D. Van Thourhout, and R. Baets, *IEEE J. Sel. Top. Quantum Electron.* **16**, 316 (2010).
- <sup>10</sup>S. K. Selvaraja, P. Jaenen, W. Bogaerts, D. Van Thourhout, P. Dumon, and R. G. Baets, *J. Lightwave Technol.* **27**, 4076 (2009).
- <sup>11</sup>D. Taillaert, P. Bienstman, and R. Baets, *Opt. Lett.* **29**, 2749 (2004).
- <sup>12</sup>F. G. Della Corte, M. E. Montefusco, L. Moretti, I. Rendina, and A. Rubino, *Appl. Phys. Lett.* **79**, 168 (2001).